Magnetic Fluctuations of Stripes in the High Temperature Cuprate Superconductors

G. Seibold[1] and J. Lorenzana[2]

[1]*Institut für Physik, BTU Cottbus, Post Box 101344, 03013 Cottbus, Germany*

[2]*SMC-INFM,ISC-CNR, Dipartimento di Fisica, Università di Roma La Sapienza, P. Aldo Moro 2, 00185 Roma, Italy*

(Received 12 July 2004; published 18 March 2005)

Within the time-dependent Gutzwiller approximation for the Hubbard model we compute the magnetic fluctuations of vertical metallic stripes with parameters appropriate for $La_{1.875}Ba_{0.125}CuO_4$ (LBCO). For bond- and site-centered stripes the excitation spectra are similar, consisting of a low-energy incommensurate acoustic branch which merges into a ''resonance peak'' at the antiferromagnetic wave vector and several high-energy optical branches. The acoustic branch is similar to the result of theories assuming localized spins whereas the optical branches are significantly different. Results are in good agreement with a recent inelastic neutron study of LBCO.

DOI: 10.1103/PhysRevLett.94.107006 PACS numbers: 74.25.Ha, 71.28.+d, 71.45.Lr, 74.72.–h

Since the discovery of cuprate superconductors the elucidation of their magnetic properties has been a subject of intense research in the high-T_c community due to their possible relevance for the superconducting mechanism [1]. However, no consensus has been reached yet on whether the magnetic excitation spectra in the various cuprate materials can be traced back to some universal phenomenology which could be expected in the face of the robust nature of superconductivity. The insulating parent compounds show long-range antiferromagnetic (AFM) order in the CuO_2 planes below the Néel temperature [2]. This static AFM order is lost above a concentration of added holes per planar copper $x \approx 0.02$, but complex dynamical spin correlations persist up to the overdoped regime [1,3].

Regarding the lanthanum cuprates (LCO), neutron scattering (NS) experiments have revealed low-energy incommensurate magnetic excitations at wave vectors (hereafter in units of $2\pi/a$ [4]) $(1/2 \pm \epsilon, 1/2)$ and $(1/2, 1/2 \pm \epsilon)$ [5] in the doping regime where the material is superconducting ($x > 0.05$). The incommensurability ϵ depends linearly on doping $\epsilon = x$ up to $x \approx 1/8$ and stays constant beyond [3]. This behavior can be successfully explained [6–8] by metallic, self-organized quasi-one-dimensional structures called stripes [9] which are oriented parallel to the Cu-O bond (hereafter vertical stripes) and act as antiphase domain walls for the antiferromagnetic order. The strongest experimental support for the stripe scenario stems from neutron [10,11] and x-ray scattering [12] experiments on LCO where codopants induce a pinning of the stripes so that the associated charge order can be detected.

In $YBa_2Cu_3O_{6+y}$ (YBCO) incommensurate magnetic fluctuations have been detected by inelastic NS (INS) [13–16] with a similar doping dependence of the low-energy incommensurability to that of LCO [15]. Upon increasing energy the incommensurate branches continuously disperse towards the so-called resonance mode at wave vector $Q_{\mathrm{AFM}} = (1/2, 1/2)$, a collective magnetic mode that grows up below T_c [17–19]. The energy E_r of the spin resonance seems to scale linearly with T_c which has led to speculations that it could be related to the superconducting pairing and phase coherence (cf. Refs. [20,21] and references therein), thus suggesting a magnetic origin of the high transition temperatures of cuprates. Finally above E_r the magnetic fluctuations in YBCO acquire again an incommensurate structure [14,16,22–24] and are already observed above T_c [16].

Very recent experiments were dedicated to explore the problem of universality in the magnetic excitations between different cuprate families [23,25–27]. In particular, Tranquada *et al.* [27] reported INS measurements of the magnetic excitations in $La_{1.875}Ba_{0.125}CuO_4$ which show static charge *and* spin order. Most interestingly the dispersion of spin excitations shows features which resemble closely those of YBCO although the measurement has been performed above T_c. The similarity between both compounds has been further demonstrated by a high-energy study of YBCO [16] and a high resolution experiment on optimally doped LCO [26]. These works [16,23,25–27] are certainly an important step towards a unified understanding of magnetic fluctuation in cuprates. On the other hand, they open new questions. The spin excitations in YBCO are commonly explained in terms of an itinerant picture as arising from a dispersing two-particle bound state induced by AFM correlations in a d-wave superconducting system [25,28]. On the other hand, magnetic excitations on top of stripes are usually described in a localized moment picture within spin-wave theory (LSWT) [29,30]. If the origin of magnetic excitations in cuprates is universal, what picture is more appropriate? The spectra of LSWT are difficult to reconcile with several features of YBCO [16,23,25] and LCO [26,27], challenging the stripe interpretation itself [23,26]. Here we show that the magnetic excitations in $La_{1.875}Ba_{0.125}CuO_4$ (and possibly in the other cuprates) can be understood in terms of the spin fluctuations of metallic stripes which are in an intermediate regime, i.e., neither the localized nor the itinerant picture applies. Contrary to the LSWT computations [29], our results are in agreement with experiment [27] over the whole range of energies and momenta.

Our investigations are based on the one-band Hubbard model (on-site repulsion U) with hopping restricted to nearest ($\sim t$) and next-nearest ($\sim t'$) neighbors. Applying the unrestricted Gutzwiller approximation (GA) as in Ref. [8], static charge and spin textures are obtained by minimizing the corresponding energy functional. The advantage of the GA in the present context is that our saddle point solutions reproduce several features of experiments [7,8] while the same would not be true if the starting point were Hartree-Fock (HF) for which stripes are not even the ground state for realistic parameters [8].

Dynamical properties are computed on top of the inhomogeneous solutions within the time-dependent GA [31] (TDGA). This scheme allows for the calculation of random-phase-approximation (RPA) fluctuations in a similar manner as the traditional HF plus RPA. At the same time it starts from a solution which incorporates correlations already at mean-field level. The TDGA has previously been shown to provide an accurate description of the optical conductivity within the more realistic three-band model [32]. Here, because we restrict our study to low-energy magnetic excitations, we do not expect that interband effects will play an important role and therefore a one-band description should be sufficient.

Parameters were fixed by requiring that (i) the linear concentration of added holes is $1/(2a)$ according to experiment [3,10,27] and (ii) a TDGA computation of the undoped AFM insulator reproduces the experimental dispersion relation [33]. Condition (i) was shown to be very sensitive to t'/t [8], whereas condition (ii) is sensitive to U/t and t, the former parameter determining the observed energy splitting between magnons at wave vectors $(1/2, 0)$ and $(1/4, 1/4)$ [33]. Indeed, the splitting vanishes within spin-wave theory applied to the Heisenberg model which corresponds to $U/t \to \infty$. We find that both conditions are met by $t'/t = -0.2$, $U/t = 8$, and $t = 354$ meV. In this way all parameters are fixed and the subsequent computation of the magnetic fluctuation of the stripes can be considered without free parameters. Results shown below are obtained in a 40×40 sites lattice and for doping $x = 1/8$ corresponding to a period of charge modulation $d = 4a$.

Since we are in an intermediate parameter regime, and also thanks to a better treatment of correlations than in HF (cf. Ref. [8]), our saddle point solutions have weak charge modulations and are metallic. This is in contrast with the traditional stripe picture [10] which is underlying the LSWT computations [29,30]. On the other hand, our solutions break the symmetry of the lattice and incorporate stripe correlations from the outset in contrast with the isotropic, itinerant picture [25,28].

The local magnetization of bond-centered (BC) stripes is reduced to 0.20 (0.38) with respect to $1/2$ inside (outside) the core of the charge domains. The band structure is quasi-one-dimensional with a Fermi momentum $k_F \sim 1/8$. Bond-centered and site-centered (SC) stripes are almost degenerate in energy, which is also found in other one-band calculations [6,34] and within the three-band model at higher doping [7,32]. We anticipate that for both structures the magnetic excitation spectra are rather similar [see Fig. 1(c)] with differences regarding the intensity distribution and gaps between magnetic bands. For definiteness we mainly restrict ourselves to the BC case because of marginally better agreement with experiment (see below). Additionally, these textures constitute the more stable configuration at $x = 1/8$ in the more accurate three-band model [7] and in first principle computations [35].

We compute the transverse dynamical structure factor, $S^{\perp}(\omega, \mathbf{q}) = \frac{(g\mu_B)^2 \eta Z_d}{N\hbar} \sum_{\nu} |\langle 0|S^{+}_{\mathbf{q}}|\nu\rangle|^2 \delta(\omega - \omega_{\nu})$, which is probed by INS. Here $g = 2$ and as in LSWT we included the renormalization factor Z_d [2]. In the insulating phase our spectral weights are close to LSWT and therefore we adopt $Z_d = 0.51$ [33]. η takes into account polarization factors in the NS cross section and will be discussed below. Energy is sampled at intervals of 3.5 meV.

A contour level plot of $\omega S^{\perp}(\omega, \mathbf{q})$ [Figs. 1(a) and 1(b)] shows the dispersion of magnetic excitations for stripes oriented along the y axis. The lower (acoustic) branch perpendicular to the stripes [1(b)] is similar to the lowest branch found within LSWT [29]. Indeed, since the acoustic branch involves long-wavelength excitations, it should not depend on the short-range details of the model. It shows the correct Goldstone-like behavior going to zero frequency at the ordering wave vector $Q_s = (1/2 \pm \epsilon, 1/2)$ with $\epsilon = 1/8$. Starting from Q_s one observes two branches of spin waves where the one dispersing towards smaller q_x rapidly loses intensity. The other one remains very intense up to Q_{AFM}, where it can be associated with the resonance peak. Moreover, as shown in Figs. 1(a) and 1(b) the dispersion develops a local maximum at Q_{AFM} explaining the strong intensity in the momentum integrated structure factor [Fig. 1(c)] at the resonance frequency. In the direction of

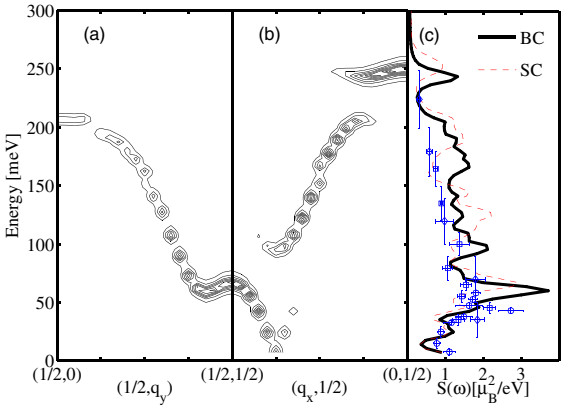

FIG. 1 (color online). Ten contour levels of $\omega S^{\perp}(\omega, \mathbf{q})$ at integer values showing the dispersion of magnetic excitations along (a) and perpendicular (b) to an array of bond-centered (BC) stripes. The factor of ω serves to cancel an infrared intensity divergence. (c) shows $S(\omega, \mathbf{q})$ integrated on the magnetic Brillouin zone around $(1/2, 1/2)$ [38] for BC and site-centered (SC) stripes together with the experimental data [27]. For the meaning of "error" bars see Ref. [27].

the stripe the excitations display a "rotonlike" minimum. The energy of the resonance at Q_{AFM} is $E_r = 65$ meV, which is reasonably close to the experimental one for this system $E_r = 55$ meV [27] taking into account the simplicity of the model and the fact that we have no free parameters.

In order to compare with experiments one should average over the two possible orientations of the stripes. In Fig. 1 this amounts to adding to each of the panels [1(a) and 1(b)] the data of the other panel reflected with respect to the central axes. One obtains an X-shaped dispersion providing a natural explanation for the X-like feature seen in both YBCO [14,24,25] and LCO [27].

The acoustic branch and its continuation in Fig. 1(a) are quite similar to the dispersion obtained in a weakly coupled two-leg ladder system [36]. In these approaches parameters are adjusted to drive the system into the quantum critical point separating the quantum paramagnet from the magnetically ordered state [37]. Hence the similarity with our spectra is reasonable since regarding the magnetism the ordered state corresponds to the present ground state and one can expect continuity of the excitations at the transition. The spin-leg ladder theories [36], however, rely heavily on the fine-tuning of the coupling parameter between the legs and an even charge periodicity of the stripes (as for $\epsilon = 1/8$). In contrast we obtain qualitatively similar spectra for $\epsilon = 1/8$ and $\epsilon = 1/10$ ($x = 0.1$, $d = 5a$) [7,8], in accord with experiment [26]. Note that this does not exclude the interesting possibility that a small spin gap opens by the ladder mechanism for $x \geq 1/8$ and $\epsilon = 1/8$ [35–37].

Above the acoustic branch in Fig. 1(b) there are three optical branches. The lowest two almost touch at $q_x = 1/4$. Gap positions are in agreement with LSWT, but the dispersion is not. Indeed the computations in Ref. [29] yield a shift of the two lower optical branches by $1/8$ along q_x with respect to our computation. Formally this difference can be traced back to the nonlocal nature of magnetic excitations in our system which shows magnetic moments considerably smaller than in the insulator, and more importantly is metallic. In LSWT only processes of the kind $S_i^+ S_j^-$ are allowed in the effective interaction kernel with i and j being close neighbors [29]. We find that not only processes with i far from j are important but also processes of the kind $c_{i,\uparrow}^\dagger c_{i',\downarrow} c_{j,\downarrow}^\dagger c_{j',\uparrow}$ with all four sites different.

The absolute spectral weights are determined by the parameter η. If one assumes a three-dimensional isotropic distribution of magnetic domains $\eta = 2/3$. If instead the magnetization is parallel to the Cu-O plane, η will decrease with energy and take values closer to $1/2$. We adopt for η 80% of the isotropic value, which gives good account of the lower part of the spectra. (At higher energies a further decrease is expected [38]).

Some details of the relative spectral weight are better reproduced by BC stripes. (i) The resonance energy E_r is closer to the experimental value in the BC case. (ii) For BC stripes the gap between the acoustic branch and the first optical branch produces a dip in the integrated intensity at 80 meV followed by a peak at 100 meV, which is in agreement with experiment contrary to the SC case. Although these features favor BC stripes, more theoretical and experimental work is needed to confirm this finding.

Figure 2 reports constant frequency scans of $S^\perp(\omega, \mathbf{q})$. At the lowest energy for y-axis oriented stripes [2(a), left] one intersects the Goldstone mode close to the incommensurate wave vector Q_s. At higher energy [2(b) and 2(c)] one intersects the spin-wave cone. The intensity is very anisotropic along the intersection and only the region closest to Q_{AFM} is visible. This effect is also apparent from Fig. 1. Although our study focuses on an underdoped system, the large intensity difference fits nicely with the fact that only the branch closest to Q_{AFM} is seen in a recent high resolu-

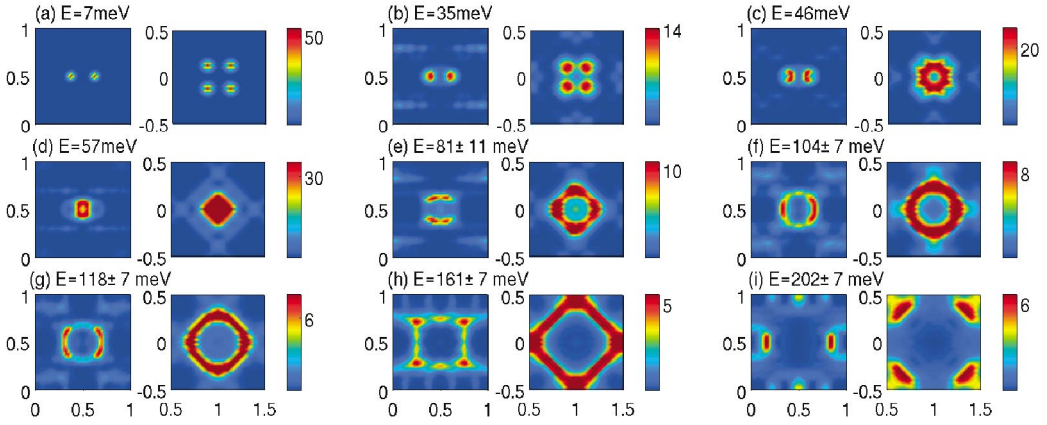

FIG. 2 (color). Constant frequency scans of $S^\perp(\omega, \mathbf{q})$ for BC stripes convolved with a Gaussian (FWHM = 0.06 reciprocal lattice units). The title indicates the energy or the energy window (e)–(i) over which intensities are averaged. For each figure (a)–(i) the left panel shows the intensity for stripes oriented along the y direction (divided by 2). In order to compare with the experimental data of Ref. [27] the right panel shows the average of both horizontal and vertical stripes with the coordinate system rotated by 45° with wave vector units of $2\pi/(\sqrt{2}a)$. Parameters are as in Fig. 1 and as explained in the text.

tion study on optimally doped LCO [26]. Immediately below the resonance [Fig. 2(d)] the spin excitations have shifted close to Q_{AFM} and one observes the appearance of intensity in the stripe direction due to the rotonlike behavior. At 81 meV one intersects the first gap of Fig. 1(b) so that the main features are due to excitations along the stripes. At higher energies the contributions from the modes perpendicular to the stripe become gradually more important. Moreover, the orientation averaged scans are in remarkably good agreement with the corresponding panels of Ref. [27].

Another very interesting finding is the horizontal cigarlike features seen at 35 meV and higher energies. Similar features have been obtained in weak coupling in the longitudinal channel [39]. These structures appear close to $q_y \sim 1/4 \sim 2k_F$ and correspond to spin-flip backscattering processes of the quasi-one-dimensional metallic subsystem. At this q_y the continuum extends to about 100 meV. As expected there is also a sharp collective mode corresponding to forward scattering processes but with too weak intensity to be observable in Fig. 2. Diffusive scattering revealed a similar phenomenon in $La_{5/3}Ni_{1/3}O_4$, where stripes are insulating but have a spin-1/2 degree of freedom at the core [40].

In conclusion, we have calculated the magnetic excitations in the stripe phase of cuprates within the TDGA applied to an extended Hubbard model. From a methodological point of view the present work together with our previous study (Ref. [32]) shows that TDGA is accurate and simple enough in order to obtain realistic dynamical properties of textured strongly correlated system. Stripes in our computation are metallic charge and spin density waves in a regime intermediate between localized moment and itinerant pictures. Our results are in good agreement with experiments in $La_{1.875}Ba_{0.125}CuO_4$ providing a straightforward explanation of the energy and momentum dependent evolution of $S^{\perp}(q, \omega)$ in terms of stripes and hence confirming stripes as a robust feature of this system with a firm theoretical basis. The fact that the magnetic excitation spectra are similar in different cuprate families and for different doping levels suggests that stripes or the proximity to stripe instabilities are a universal property of cuprates and hence that they may be relevant for the superconducting mechanism.

We acknowledge invaluable insight from J. M. Tranquada, A. T. Boothroyd, and R. Coldea. G. S. acknowledges financial support from the Deutsche Forschungsgemeinschaft.

[1] M. A. Kastner *et al.*, Rev. Mod. Phys. **70**, 897 (1998).
[2] E. Manousakis, Rev. Mod. Phys. **63**, 1 (1991).
[3] K. Yamada *et al.*, Phys. Rev. B **57**, 6165 (1998).
[4] $a \sim 3.8$ Å is the lattice spacing in tetragonal coordinates.
[5] S-W. Cheong *et al.*, Phys. Rev. Lett. **67**, 1791 (1991).
[6] M. Fleck *et al.*, Phys. Rev. Lett. **84**, 4962 (2000); M. Fleck, A. I. Lichtenstein, and A. M. Oleś, Phys. Rev. B **64**, 134528 (2001).
[7] J. Lorenzana and G. Seibold, Phys. Rev. Lett. **89**, 136401 (2002)
[8] G. Seibold and J. Lorenzana, Phys. Rev. B **69**, 134513 (2004).
[9] J. Zaanen and O. Gunnarsson, Phys. Rev. B **40**, R7391 (1989); K. Machida, Physica (Amsterdam) **158C**, 192 (1989); H. J. Schulz, Phys. Rev. Lett. **64**, 1445 (1990); D. Poilblanc and T. M. Rice, Phys. Rev. B **39**, R9749 (1989).
[10] J. M. Tranquada *et al.*, Nature (London) **375**, 561 (1995).
[11] M. Fujita *et al.*, Phys. Rev. B **70**, 104517 (2004).
[12] T. Niemöller *et al.*, Eur. Phys. J. B **12**, 509 (1999).
[13] H. A. Mook *et al.*, Nature (London) **395**, 580 (1998).
[14] M. Arai *et al.*, Phys. Rev. Lett. **83**, 608 (1999).
[15] Pengcheng Dai *et al.*, Phys. Rev. B **63**, 054525 (2001).
[16] S. M. Hayden *et al.*, Nature (London) **429**, 531 (2004).
[17] J. Rossat-Mignod *et al.*, Physica (Amsterdam) **185–189C**, 86 (1991).
[18] H. F. Fong *et al.*, Phys. Rev. Lett. **75**, 316 (1995).
[19] P. Bourges *et al.*, Phys. Rev. B **53**, 876 (1996).
[20] Pengcheng Dai *et al.*, Science **284**, 1344 (1999).
[21] Pengcheng Dai *et al.*, Nature (London) **406**, 965 (2000).
[22] M. Arai *et al.*, Int. J. Mod. Phys. B **14**, 3312 (2000).
[23] D. Reznik *et al.*, Phys. Rev. Lett. **93**, 207003 (2004).
[24] H. A. Mook, P. Dai, and F. Dogan, Phys. Rev. Lett. **88**, 097004 (2002).
[25] S. Pailhes *et al.*, Phys. Rev. Lett. **93**, 167001 (2004).
[26] N. B. Christensen *et al.*, Phys. Rev. Lett. **93**, 147002 (2004).
[27] J. M. Tranquada *et al.*, Nature (London) **429**, 534 (2004).
[28] J. Brinckmann and P. A. Lee, Phys. Rev. Lett. **82**, 2915 (1999); Ying-Jer Kao, Qimiao Si, and K. Levin, Phys. Rev. B **61**, R11898 (2000); M. R. Norman, Phys. Rev. B **61**, 14 751 (2000); F. Onufrieva and P. Pfeuty, Phys. Rev. B **65**, 054515 (2002).
[29] C. D. Batista, G. Ortiz, and A. V. Balatsky, Phys. Rev. B **64**, 172508 (2001); F. Krüger and S. Scheidl, Phys. Rev. B **67**, 134512 (2003); E. W. Carlson, D. X. Yao, and D. K. Campbell, Phys. Rev. B **70**, 064505 (2004).
[30] A. T. Boothroyd *et al.*, Phys. Rev. B **67**, 100407(R) (2003).
[31] G. Seibold and J. Lorenzana, Phys. Rev. Lett. **86**, 2605 (2001); G. Seibold, F. Becca, and J. Lorenzana, Phys. Rev. B **67**, 085108 (2003); G. Seibold *et al.*, Phys. Rev. B **69**, 155113 (2004).
[32] J. Lorenzana and G. Seibold, Phys. Rev. Lett. **90**, 066404 (2003).
[33] R. Coldea *et al.*, Phys. Rev. Lett. **86**, 5377 (2001).
[34] S. R. White and D. J. Scalapino, Phys. Rev. Lett. **80**, 1272 (1998); G. B. Martins *et al.*, Phys. Rev. Lett. **84**, 5844 (2000).
[35] V. I. Anisimov *et al.*, Phys. Rev. B **70**, 172501 (2004).
[36] M. Vojta and T. Ulbricht, Phys. Rev. Lett. **93**, 127002 (2004); G. S. Uhrig, K. P. Schmidt, and M. Grüninger, Phys. Rev. Lett. **93**, 267003 (2004).
[37] S. Sachdev, Rev. Mod. Phys. **75**, 913 (2003).
[38] J. M. Tranquada (private communication).
[39] E. Kaneshita, M. Ichioka, and K. Machida, J. Phys. Soc. Jpn. **70**, 866 (2001).
[40] A. T. Boothroyd *et al.*, Phys. Rev. Lett. **91**, 257201 (2003).